

Shape resonances in the electron-hydrogen system with screened Coulomb potentials

L. G. Jiao* and Y. K. Ho†

Institute of Atomic and Molecular Sciences, Academia Sinica, P.O. Box 23-166, Taipei 106, Taiwan

(Received 17 January 2013; published 15 May 2013)

We investigate the shape resonances of the electron-hydrogen system embedded in Debye plasma environments modeled by screened Coulomb potentials. The complex-coordinate rotation method is employed to calculate the resonance parameters and the Hylleraas-type wave functions are used to represent the correlation effects of the two electrons. The $1S^e$ resonance states of H^- above the $N = 2-5$ thresholds of H atom are investigated and the resonance parameters for a Debye length ranging from infinity to small values are reported. It is shown that the widths of the shape resonances lying above the $H(N = 4,5)$ thresholds exhibit some interesting behaviors in relatively strong screening situations. The possible reason for such phenomena is discussed.

DOI: [10.1103/PhysRevA.87.052508](https://doi.org/10.1103/PhysRevA.87.052508)

PACS number(s): 31.15.vj, 32.80.Zb, 52.20.Fs

I. INTRODUCTION

The investigation of resonance phenomena in electron-hydrogen systems with screened Coulomb potentials has gained considerable attention due to its important applications in various aspects of atomic physics, plasma physics, and astrophysics [1–4]. For example, the screened Coulomb potentials can be used to describe the weakly coupled plasmas in the Debye-Hückel model. The screening parameter is referred to as the Debye length D , which is related to the temperature and the number density of the charged particles in plasmas [5]. In the past few years, several theoretical methods have been used by different groups to calculate the Feshbach resonances in the electron-hydrogen system with screened Coulomb potentials such as the stabilization method initiated by Kar and Ho [6–8], the close-coupling approximation employed by Basu [9–11], the R -matrix method with pseudostates introduced by Zhang *et al.* [12–14], and the complex-coordinate rotation method by Ho and co-workers [15,16]. In addition, the scattering of the electron-hydrogen system in Debye plasmas and the photodetachment processes of H^- embedded in weakly coupled and dense quantum plasmas have also been investigated by other authors [17–20] and abundant phenomena have been found.

Although there is considerable work on Feshbach resonances of H^- with screening environments, investigations on shape resonances are scarce. The formations of Feshbach and shape resonances in the scattering of electron and hydrogen are based on different underlying mechanisms. The shape resonances, which are also called open-channel resonances, depict the electron tunneling through a potential barrier formed by the nonzero angular momentum of the electron, remaining confined inside the barrier for the lifetime of the resonance, and then tunneling out. The Feshbach resonances, or the closed-channel resonances, are formed when the electron is temporarily trapped by the potential well formed by the attractive static and polarization potentials between the electron and excited target. The shape resonances generally lie above the corresponding thresholds and have larger widths, whereas the Feshbach resonances always lie below the thresholds and have smaller widths. Details of the classification of

shape and Feshbach resonances have been given previously [21,22]. For the unscreened case where only pure Coulomb interactions exist, the shape resonances of the H^- system have been extensively investigated in the past few decades both theoretically and experimentally (see [23–26] and references therein). A detailed analysis of S - and P -wave shape and Feshbach resonances in H^- was presented by Bürgers and Lindroth [27] using the complex-coordinate rotation method with a Sturmian-type basis in perimetric coordinates. The Feshbach resonances were well classified by approximate group-theoretic quantum numbers ${}_N(K, T)_n^A$ [28]. It is also worth mentioning here that recently the lowest S -wave shape resonances of H^- were investigated by Kar and Ho [29] and interesting results were obtained by tracing the shape resonance pole from H^- to Ps^- via changing the mass of the target nucleus.

In this work we focus our attention on the singlet- S -wave shape resonances of electron-hydrogen system in the Debye model plasmas described by the screened Coulomb potentials. Due to the different formation mechanism and possible autoionization routes between the shape and Feshbach resonances, Debye plasmas may have different screening effects on the resonance parameters. Therefore, the investigations of shape resonances are supplementally important for a full understanding of the electron correlations and plasma screening effects for multielectron atoms. In the present calculation, the complex-coordinate rotation method [30,31] is employed to extract the $1S^e$ shape resonance parameters. The highly correlated Hylleraas-type basis functions are used to construct the system wave functions and the electron-electron correlations can be taken into account properly. The convergence of our calculations has been achieved by increasing the numbers of Hylleraas basis functions. Atomic units are used throughout the work.

II. CALCULATIONS

The nonrelativistic Hamiltonian describing the negative hydrogen ion in the screening environments is given by

$$H = -\frac{1}{2}\nabla_1^2 - \frac{1}{2}\nabla_2^2 - \frac{\exp(-r_1/D)}{r_1} - \frac{\exp(-r_2/D)}{r_2} + \frac{\exp(-r_{12}/D)}{r_{12}}, \quad (1)$$

*lgjiao@pub.iams.sinica.edu.tw

†ykho@pub.iams.sinica.edu.tw

where r_1 and r_2 are the radial coordinates of the two electrons from the hydrogen nucleus and r_{12} is the relative distance between the electrons. The screening parameter D is the Debye length, which characterizes the range of the plasmas. The infinite value of D corresponds to the free-atom situation, whereas the smaller value of D represents strong screening effects. In the present calculation, the screened Coulomb potential is approximated by using the Taylor expansion

$$\frac{\exp(-r_{ij}/D)}{r_{ij}} = \sum_{n=0}^m (-1)^n \frac{r_{ij}^{n-1}}{D^n n!}, \quad (2)$$

where r_{ij} is the radial coordinate between any pairs of charged particles i and j , with i and j the electrons or the nucleus. In Eq. (2) $m = 0$ indicates the pure Coulomb interactions and $m > 0$ represents the first-, second-, and higher-order perturbations of screening effects on the Coulomb interaction. In the present calculation, an extensive expansion of $m = 18$ throughout our work (the order for $1/D$ up to the power of 18) is used and the smallest value for D is restricted to 10 a.u. ($1/D = 0.1$). It is therefore believed that keeping the lowest 19 terms of the Taylor series in the expansion would be reasonably accurate for the problems investigated here.

For the S -wave states we use the Hylleraas-type wave functions to describe the system

$$\Psi_{klm}(r_1, r_2) = \sum_{klm} C_{klm} e^{-\alpha(r_1+r_2)} r_{12}^k (r_1^l r_2^m + r_2^l r_1^m), \quad (3)$$

with $k + l + m \leq \omega$, where k, l, m , and ω are positive integers or zero and α is the nonlinear scaling parameter. In the present work we have performed calculations with $\omega = 18, 19, 20$, and 21 separately, which couple to total of 715, 825, 946, and 1078 terms in the system wave functions, respectively, to examine the convergence behaviors of our calculations.

The complex-coordinate rotation method is employed to extract the resonance parameters. The radial coordinates are rotated through an angle of θ ,

$$r \rightarrow |r|e^{i\theta}. \quad (4)$$

The Hamiltonian of the system is then transformed into

$$H(\theta) = T e^{-2i\theta} + V'(\theta), \quad (5)$$

where T is the kinetic energy operator and the potential $V'(\theta)$ reads

$$-\frac{\exp(-r_1 e^{i\theta}/D)}{r_1 e^{i\theta}} - \frac{\exp(-r_2 e^{i\theta}/D)}{r_2 e^{i\theta}} + \frac{\exp(-r_{12} e^{i\theta}/D)}{r_{12} e^{i\theta}}. \quad (6)$$

Under the complex scaling, the potential operators in the form of Eq. (2) would be scaled like

$$\frac{\exp(-r_{ij} e^{i\theta}/D)}{r_{ij} e^{i\theta}} = \sum_{n=0}^m (-1)^n \frac{r_{ij}^{n-1}}{D^n n!} e^{i(n-1)\theta}. \quad (7)$$

We calculate the matrix elements $\langle r_{ij}^{n-1} \rangle$ for $n = 0$ and $2 \leq n \leq 18$ analytically. These matrix elements are then multiplied by the scaling factor $e^{i(n-1)\theta}$, respectively, for different n . The final θ -dependent matrix elements for the potential operators can be constructed by combining all the θ -dependent matrix elements for various expectation values of r_{ij} factors.

Due to the fact that the Hylleraas-type wave functions are nonorthogonal basis functions, the complex eigenvalue problem is solved with

$$\sum_j C_j^\lambda (H_{ij} - E^\lambda N_{ij}) = 0, \quad (8)$$

in which

$$H_{ij} = \langle \psi_i | H(\theta) | \psi_j \rangle \quad (9)$$

and the overlapping matrix

$$N_{ij} = \langle \psi_i | \psi_j \rangle. \quad (10)$$

The resonances are determined by finding the position where the complex eigenvalues exhibit the most stabilized character with respect to the changes of rotation angle θ , the nonlinear scaling parameter α , and the expansion length of the resonant wave function [31]

$$\left. \frac{\partial |E_{\text{res}}|}{\partial \theta} \right|_{\alpha=\alpha_{\text{opt}}} = \min, \quad \left. \frac{\partial |E_{\text{res}}|}{\partial \alpha} \right|_{\theta=\theta_{\text{opt}}} = \min. \quad (11)$$

Once the position of the pole is determined, the resonance energy E_r and total width Γ are given by

$$E_{\text{res}} = E_r - \frac{1}{2}i\Gamma. \quad (12)$$

TABLE I. Convergence of the present calculations using different expansion lengths of basis sets at $D = \infty$ and comparisons with previous complex-scaling calculations using different kinds of bases. Half of the total width ($\Gamma/2$) is used for convenience. All the results are given in atomic units.

ω	M	$\text{H}^-(N=2)$		$\text{H}^-(N=3)$		$\text{H}^-(N=4)$		$\text{H}^-(N=5)$	
		E_r	$\Gamma/2$	E_r	$\Gamma/2$	E_r	$\Gamma/2$	E_r	$\Gamma/2$
18	715	-0.103035727	0.015627345	-0.03544006	0.00813109	-0.0285491	0.00131957	-0.0168706	0.0012751
19	825	-0.103035664	0.015627309	-0.03543887	0.00813107	-0.0285507	0.00131951	-0.0168850	0.0012726
20	946	-0.103035685	0.015627314	-0.03543916	0.00813108	-0.0285505	0.00131835	-0.0168845	0.0012672
21	1078	-0.103035677	0.015627312	-0.03543900	0.00813104	-0.0285501	0.00131871	-0.0168847	0.0012678
		-0.103035676 ^a	0.015627312 ^a	-0.03543901 ^a	0.00813107 ^a	-0.0285503 ^a	0.00131876 ^a	-0.0168848 ^a	0.0012685 ^a
		-0.10303569 ^b	0.01562729 ^b						
		-0.1030357 ^c	0.0156273 ^c						

^aSturmian-type basis [27].

^bHylleraas-type basis [29].

^cExponential correlated basis [29].

III. RESULTS AND DISCUSSION

We have examined the convergence of our calculations. The shape resonances that lie above the $H(N = 2, 3, 4, 5)$ thresholds at $D = \infty$ are calculated with $\omega = 18, 19, 20, 21$, respectively. To find the stabilized character of the complex eigenvalue, calculations are performed by varying the rotational angle θ from 0.3 to 0.9 rad at intervals of 0.02 rad and the nonlinear scaling parameter α from 0.02 to 0.50 at intervals of 0.02. All the results are shown in Table I. Previous complex-scaling calculations employing a Sturmian-type basis by Bürgers and Lindroth [27] and exponential-correlated and Hylleraas wave functions by Kar and Ho [29] are also included for comparison. It can be seen that the convergence of the present calculations improves with increasing size of the basis set and the results with $\omega = 21$ are in excellent agreement with the elaborate calculations of Bürgers and Lindroth with the Sturmian-type basis [27]. For the lowest $H^-(N = 2)$ shape resonance, the present results are closer to the results in Ref. [27] than those of Ref. [29].

In Fig. 1(a) we have displayed the $1S^e$ shape resonances in the present calculations and the Feshbach resonances predicted

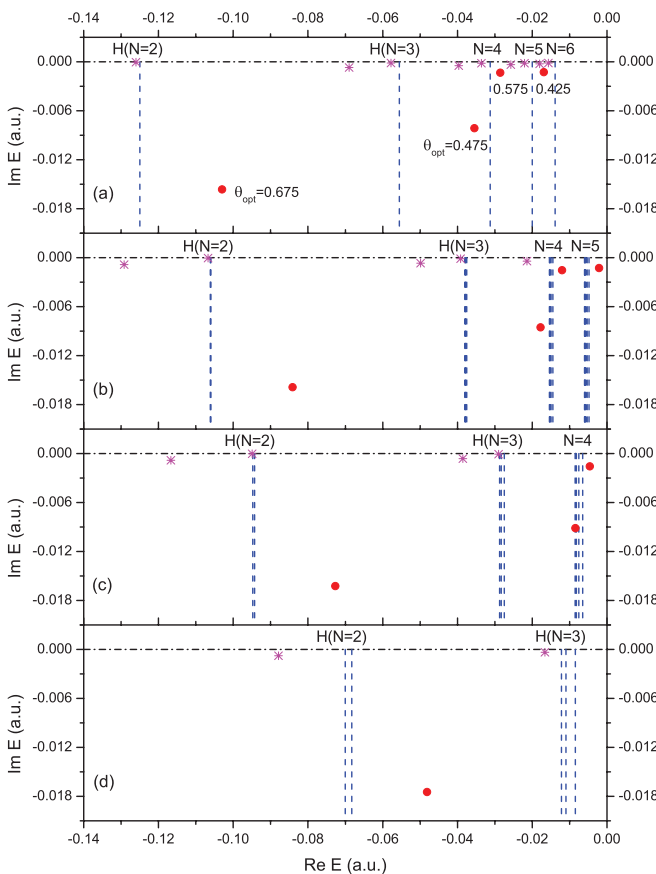


FIG. 1. (Color online) The $1S^e$ shape resonances of H^- above the $H(N = 2-5)$ thresholds in the complex energy plane with different Debye lengths D : (a) $D = \infty$, (b) $D = 50$, (c) $D = 30$, and (d) $D = 15$. The dash lines (blue) represent the thresholds of H [32]. The solid circles (red) refer to the shape resonances lying above the corresponding thresholds in the present calculations. The stars (magenta) are the Feshbach resonances lying below the thresholds predicted in previous work [6,15,16,27].

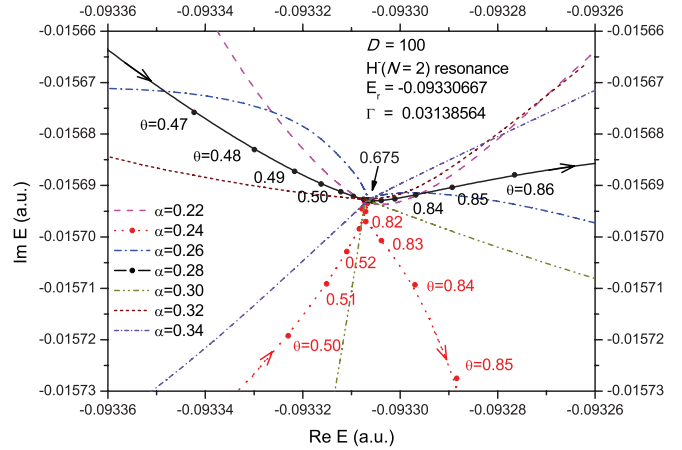


FIG. 2. (Color online) Rotational paths for the $H^-(N = 2)$ shape resonances at $D = 100$ for a set of scaling parameters $\alpha = 0.22-0.34$. Each line represents a single value of α with different rotational angle $\theta \approx 0.40-0.90$. Two rotational paths ($\alpha = 0.24$ and 0.28) are shown in detail. The (black) solid line refers to the rotational path with an optimized value of $\alpha_{\text{opt}} = 0.28$.

in previous work [6,15,16,27], as well as the corresponding H thresholds [32] in the complex energy plane. It is clear that the shape resonances generally have much larger widths than the Feshbach resonances associated with the same thresholds. The larger widths also imply that larger θ_{opt} are required in Eq. (4) to make sure that all the shape resonances can be extracted from the rotated continuum. In the present calculations, the optimized θ for $H^-(N = 2, 3, 4, 5)$ shape resonances are 0.675, 0.475, 0.575, and 0.425 rad, respectively. We show also results for the shape resonance poles in the screening environment for $D = 50, 30$, and 15 in Figs. 1(b)–1(d), respectively.

The essential procedure to extract the resonance parameters within the framework of complex-coordinate rotation can be found elsewhere. In Fig. 2 we show the rotational diagram of the $H^-(N = 2)$ shape resonance at $D = 100$ for illustrative purposes. The rotational paths for a set of scaling parameters α are displayed with different rotational angle θ . For each curve, the movement of the complex energy with increasing θ slows down (i.e., the energy is stabilized) when θ approaches $\theta_{\text{opt}} = 0.675$ rad, as described in Eq. (11). With further examination of the changes of resonance energy with respect to α at θ_{opt} , the value of $\alpha_{\text{opt}} = 0.28$ is obtained. Finally, the complex eigenvalue at θ_{opt} and α_{opt} can be used in Eq. (12) to extract the resonance parameters. In such a manner, we have calculated the lowest four shape resonances at Debye lengths from ∞ to 10 . All the results are shown in Table II. The resonance energies and the corresponding H thresholds are displayed in Figs. 3 and 4 with the change of $1/D$; the resonance widths are shown in Fig. 5.

From Figs. 3 and 4 we can see that all the resonance energies move upward with decreasing D due to the overall repulsive effect of the screened potentials. It is also very interesting to note that the shape resonances increase with a speed similar to the corresponding H thresholds, despite the splitting of hydrogen states with the same principle quantum number n in the screening environments. This reflects the height of

TABLE II. The $1S^e$ shape resonances of H^- above the $H(N = 2-5)$ thresholds for selected values of the screening parameter D . The resonance energies and widths are generally kept to six significance digits. All the results are given in atomic units.

D	$H^-(N = 2)$		$H^-(N = 3)$		$H^-(N = 4)$		$H^-(N = 5)$	
	E_r	$10^{-2}\Gamma$	E_r	$10^{-2}\Gamma$	E_r	$10^{-3}\Gamma$	E_r	$10^{-3}\Gamma$
∞	-0.1030357	3.12546	-0.0354390	1.62621	-0.0285501	2.63741	-0.0168847	2.53567
500	-0.1010465	3.12602	-0.0334629	1.62730	-0.0265850	2.64569	-0.0149406	2.53958
300	-0.0997325	3.12700	-0.0321721	1.62917	-0.0253137	2.65936	-0.0137059	2.54467
200	-0.0981035	3.12887	-0.0305882	1.63270	-0.0237683	2.68394	-0.0122303	2.55123
150	-0.0964896	3.13145	-0.0290372	1.63747	-0.0222711	2.71516	-0.0108288	2.55624
125	-0.0952092	3.13399	-0.0278198	1.64211	-0.0211081	2.74382	-0.0097599	2.55841
110	-0.0941688	3.13637	-0.0268392	1.64641	-0.0201793	2.76909	-0.0089194	2.55880
100	-0.0933067	3.13856	-0.0260326	1.65033	-0.0194210	2.79118	-0.0082422	2.55819
85	-0.0916459	3.14334	-0.0244941	1.65875	-0.0179891	2.83542	-0.0069871	2.55489
75	-0.0901837	3.14813	-0.0231566	1.66708	-0.0167607	2.87550	-0.0059368	2.55011
70	-0.0893023	3.15128	-0.0223583	1.67250	-0.0160351	2.89999	-0.0053288	2.54679
65	-0.0882915	3.15514	-0.0214499	1.67907	-0.0152164	2.92739	-0.0046549	2.54286
60	-0.0871203	3.15993	-0.0204072	1.68719	-0.0142868	2.95902	-0.0039062	2.53853
55	-0.0857475	3.16598	-0.0191987	1.69727	-0.0132228	2.99433	-0.0030733	2.53503
50	-0.0841163	3.17378	-0.0177822	1.71008	-0.0119952	3.03347	-0.0021481	2.53434
45	-0.0821465	3.18405	-0.0161001	1.72668	-0.0105667	3.07518		
40	-0.0797210	3.19796	-0.0140729	1.74884	-0.0088905	3.11610		
37	-0.0779767	3.20882	-0.0126457	1.76586	-0.0077427	3.13712		
35	-0.0766622	3.21747	-0.0115874	1.77915	-0.0069103	3.14779		
32	-0.0744120	3.23318	-0.0098110	1.80324	-0.0055518	3.15495		
30	-0.0726878	3.24599	-0.0084804	1.82265	-0.0045693	3.15082		
27	-0.0696780	3.26991	-0.0062240	1.85852	-0.0029808	3.12170		
25	-0.0673211	3.28999	-0.0045176	1.88851	-0.0018587	3.07920		
20	-0.0596975	3.36281						
17	-0.0533887	3.43166						
15	-0.0481045	3.49489						
13	-0.0416472	3.57849						
12	-0.0378691	3.63033						
11	-0.0336577	3.69033						
10	-0.0289651	3.75952						

the repulsive potential barrier related to the formation of shape resonances being nearly unchanged when changing the

screening strength. Also in Figs. 3 and 4, the degeneracies of the $H(nl)$ states with the same principle quantum number n

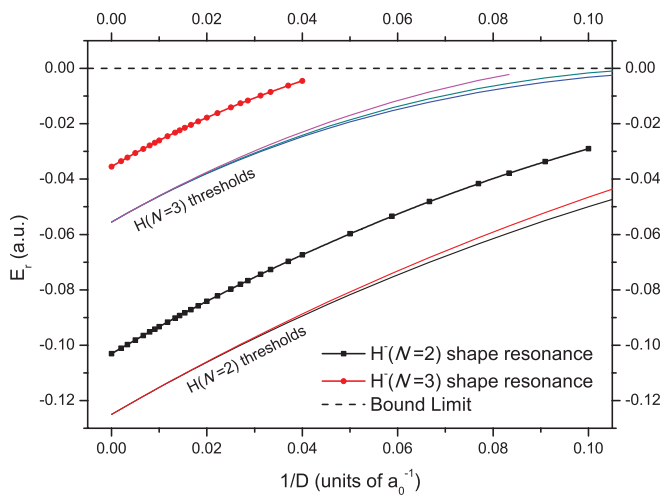


FIG. 3. (Color online) The $H^-(N = 2)1S^e$ and $H^-(N = 3)1S^e$ shape resonances and their corresponding H thresholds as a function of $1/D$: thin lines, H thresholds; dashed lines, H^- shape resonances above the thresholds. (See the text about the splitting of energy levels of the parent states in the screening environment.)

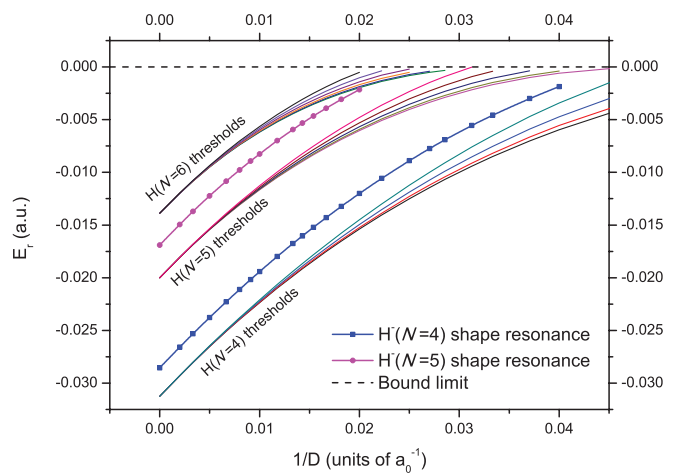


FIG. 4. (Color online) The $H^-(N = 4)1S^e$ and $H^-(N = 5)1S^e$ shape resonances and their corresponding H thresholds as a function of $1/D$. The $H(N = 6)$ thresholds are also shown for comparison. (See the text about the splitting of energy levels of the parent states in the screening environment.)

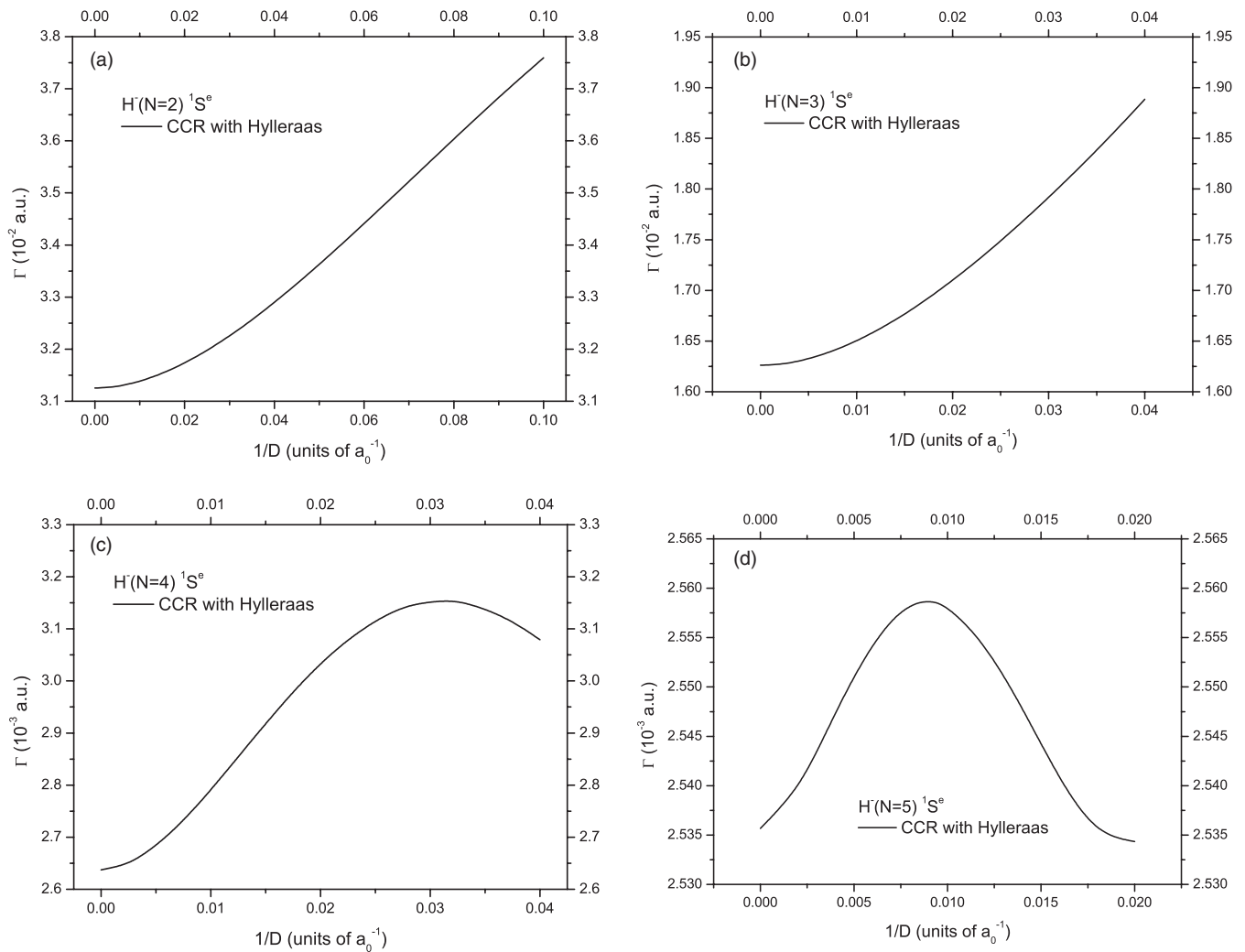


FIG. 5. Width of the $1S^e$ shape resonances in the H^- system as a function of $1/D$. The $H^-(N = 2-5)$ resonances are shown in (a)–(d), respectively.

are destroyed in the screening environment. For example, the $n = 3$ parent states (the $3s$, $3p$, and $3d$ states of the H atom) are split into three separate curves when $1/D$ is increased from zero, with the lower angular momentum states lying at lower energies, and the separation becomes more visible in the figures when $1/D$ is sufficiently large. Additionally, as we can see from Eq. (1), the long-range pure Coulomb interactions become short-range ones when the screening environments are introduced. With increasing screening strength, i.e., decreasing D , the potentials between the outer electron and the excited H atom will be compressed to a smaller region. As a result, the thickness of the potential barrier would decrease. From the above discussion that shape resonances always lie at nearly the same positions above the corresponding thresholds, the lifetime of the autoionizing electron will be shortened and the resonance width would consequently increase due to the uncertainty principle.

We show the widths of $H^-(N = 2$ and $3)$ shape resonances in Figs. 5(a) and 5(b), respectively. It can be seen that both of them increase monotonically with decreasing D in the entire region that we investigated. However, it is interesting to find that the widths of $H^-(N = 4, 5)$ shape resonances displayed

in Figs. 5(c) and 5(d) show different trends from the $H^-(N = 2, 3)$ resonances. Their widths first increase with decreasing D , reaching the maximum at $D = 32$ and 110 for $N = 4$ and 5 shape resonances, respectively, and then decrease as the value of D is further decreased. The convergence of our calculations at different Debye length D has been examined and the results are shown in Table III. Both the resonance energies and widths reported here are accurate to at least four significant digits. We present here an explanation for such phenomena. Generally, the $1S^e$ shape resonance states may have components of products with more than one angular momentum, i.e., the $n p n' p$, $n d n' d$, $n f n' f$, etc., due to the strong configuration interactions. It was also conjectured by Bürgers and Lindroth [27] that “these shape resonances are due to a [nonadiabatic] coupling between different binding and [antibinding] adiabatic potentials [that] corresponds to a mixing of ${}_N(KT)$ or $[N_1 N_2 m]$ approximate quantum numbers [28,33] where both positive and negative K would occur.” The couplings between different configurations are very strong for higher-lying resonances. As a result, the shape resonance may have more routes to autoionization. First, the shape resonance can autoionize to one of the lower-lying target states by ejecting an electron. Such a process

TABLE III. Convergence of the present calculations using different expansion lengths at $D = 100$ and 30 . All the results are given in atomic units.

$D = 100$		$H^-(N = 2)$		$H^-(N = 3)$		$H^-(N = 4)$		$H^-(N = 5)$	
ω	M	E_r	Γ	E_r	Γ	E_r	Γ	E_r	Γ
18	715	-0.09330672	0.03138572	-0.0260336	0.0165037	-0.0194219	0.00278922	-0.0082409	0.00255477
19	825	-0.09330666	0.03138563	-0.0260325	0.0165033	-0.0194212	0.00279250	-0.0082428	0.00255843
20	946	-0.09330668	0.03138565	-0.0260328	0.0165035	-0.0194210	0.00279146	-0.0082416	0.00255821
21	1078	-0.09330667	0.03138564	-0.0260326	0.0165033	-0.0194210	0.00279118	-0.0082422	0.00255819
$D = 30$		$H^-(N = 2)$		$H^-(N = 3)$		$H^-(N = 4)$			
ω	M	E_r	Γ	E_r	Γ	E_r	Γ		
18	715	-0.07268777	0.03246004	-0.0084851	0.0182461	-0.0045683	0.00315268		
19	825	-0.07268776	0.03245996	-0.0084800	0.0182303	-0.0045691	0.00315121		
20	946	-0.07268775	0.03245992	-0.0084807	0.0182312	-0.0045694	0.00315061		
21	1078	-0.07268775	0.03245991	-0.0084804	0.0182265	-0.0045693	0.00315082		

is similar to the autoionization of Feshbach resonances. It has relatively small contributions to the total width and would result in the width narrowing with increasing screening strength (see [6,7,15] for the changes of Feshbach resonance width). Second, the shape resonance would also have the probability to eject an electron, through tunneling out of the potential barrier, and autoionize to the immediately-lower-lying states of target. For example, the $H^-(N = 4)$ shape resonance can eject a P -, D -, or F -wave electron and autoionize to the $4p$, $4d$, or $4f$ excited state, respectively, of the H atom. The resonance width is largely determined by the thickness of the potential barrier. In general, the tunneling of the electron through the barrier is usually quite fast [21] and the shape resonance tends to decay into its parent state rather than into one of the lower-lying states of the H atom. This process contributes a large part to the total width and leads to the broadening of the resonance width with increasing screening environments. For the $H^-(N = 2, 3)$ shape resonances, the resonance widths are much larger than the nearby Feshbach resonances by one or two orders of magnitude. The overall effect of the screening environments on the total width is broadening. However, for the $H^-(N = 4, 5)$ shape resonances, as we can see from Fig. 1, their resonance widths are relatively small and comparable to the Feshbach resonance widths, which means that these two processes may have comparable contributions to the total width. The competition of these two effects results in the narrowing of the total width after they have reached the critical values of D .

Finally, we should also mention that there might be possible interference between the shape resonances and those Feshbach resonances associated with higher thresholds. For example, the $H^-(N = 5)$ shape resonance ($E_r = -0.0168847$) lies between the $H^-(6s6s)^1S^e$ ($E_r = -0.0180119$) and $H^-(6p6p)^1S^e$ ($E_r = -0.0166695$) Feshbach resonances [27] at $D = \infty$ and reaches a position very close to the $H(N = 6)$ thresholds at $D = 50$ (see Fig. 4). This implies that the

potential barrier associated with $H(N = 5)$ thresholds can be affected by the potential well associated with $H(N = 6)$ states. Unfortunately, we are not in a position to construct potential curves for the shape and Feshbach resonances for such high-lying states in our present investigations. Further work is needed to shed light on this open question.

IV. CONCLUSION

In the present work, we have investigated the $^1S^e$ shape resonances of H^- system embedded in Debye screening environments. Four resonances associated with and lying above the $H(N = 2-5)$ thresholds are calculated and the resonance parameters are reported from $D = \infty$ to small values. For the unscreened case, our results agree with those in Ref. [27] quite well. For the screened cases, it has been shown that the resonance energy follows a trend similar to the corresponding thresholds with increasing screening effects. The resonance widths of $H^-(N = 2, 3)$ resonances increase monotonically; however, the widths for $H^-(N = 4, 5)$ resonances show a maximum structure. The decrease of the resonance width for higher-lying shape resonances at relatively strong screening environments is probably due to the competition of two different autoionizing routes. The one describing the tunneling of the electron through potential barrier results in broadening of the width, whereas the other describing the autoionization to lower-lying thresholds results in narrowing. It seems further investigations on higher partial-wave shape resonances are worthwhile, especially for the region around high-lying H thresholds. We believe our results will provide useful references for future investigations.

ACKNOWLEDGMENT

Financial support from the National Science Council of Taiwan (Republic of China) is gratefully acknowledged.

- [1] D. Salzman, *Atomic Physics in Hot Plasmas* (Oxford University Press, Oxford, 1998).
 [2] H. R. Griem, *Principles of Plasma Spectroscopy* (Cambridge University Press, Cambridge, 2005).

- [3] M. S. Murilloa and J. C. Weisheit, *Phys. Rep.* **302**, 1 (1998).
 [4] A. N. Sil, S. Canuto, and P. K. Mukherjee, *Adv. Quantum Chem.* **58**, 115 (2009).
 [5] P. Debye and E. Hückel, *Phys. Z.* **24**, 185 (1923).

- [6] S. Kar and Y. K. Ho, *Phys. Rev. E* **70**, 066411 (2004); *New J. Phys.* **7**, 141 (2005); *Few-Body Syst.* **40**, 13 (2006).
- [7] S. Kar and Y. K. Ho, *J. Phys. B* **42**, 185005 (2009); **44**, 015001 (2011).
- [8] S. Kar and Y. K. Ho, *Phys. Rev. A* **83**, 042506 (2011).
- [9] A. Basu, *Europhys. Lett.* **88**, 53001 (2009).
- [10] A. Basu, *J. Phys. B* **43**, 115202 (2010).
- [11] A. Basu, *Eur. Phys. J. D* **61**, 51 (2011).
- [12] S. B. Zhang, J. G. Wang, and R. K. Janev, *Phys. Rev. Lett.* **104**, 023203 (2010).
- [13] S. B. Zhang, J. G. Wang, and R. K. Janev, *Phys. Rev. A* **81**, 032707 (2010).
- [14] S. B. Zhang, J. G. Wang, R. K. Janev, and X. J. Chen, *Phys. Rev. A* **83**, 032724 (2011).
- [15] S. Chakraborty and Y. K. Ho, *Chem. Phys. Lett.* **438**, 99 (2007).
- [16] Y. K. Ho and S. Kar, *Few-Body Syst.* **53**, 445 (2012).
- [17] M. C. Zammit, D. V. Fursa, and I. Bray, *Phys. Rev. A* **82**, 052705 (2010).
- [18] A. Ghoshal and Y. K. Ho, *J. Phys. B* **43**, 045203 (2010).
- [19] S. Kar and Y. K. Ho, *Phys. Plasmas* **15**, 013301 (2008).
- [20] A. Ghoshal and Y. K. Ho, *Phys. Rev. E* **81**, 016403 (2010).
- [21] G. J. Schulz, *Rev. Mod. Phys.* **45**, 378 (1973).
- [22] S. J. Buckman and C. W. Clark, *Rev. Mod. Phys.* **66**, 539 (1994).
- [23] Y. K. Ho and A. K. Bhatia, *Phys. Rev. A* **48**, 3720 (1993); Y. K. Ho, *ibid.* **49**, 3659 (1994); **50**, 4877 (1994); *Phys. Lett. A* **189**, 374 (1994).
- [24] J. Callaway, *Phys. Rev. A* **26**, 199 (1982).
- [25] A. Pathak, A. E. Kingston, and K. A. Berrington, *J. Phys. B* **21**, 2939 (1988).
- [26] J. F. Williams, *J. Phys. B* **21**, 2107 (1988).
- [27] A. Bürgers and E. Lindroth, *Eur. Phys. J. D* **10**, 327 (2000).
- [28] D. R. Herrick, *Adv. Chem. Phys.* **52**, 1 (1983).
- [29] S. Kar and Y. K. Ho, *Phys. Rev. A* **86**, 014501 (2012).
- [30] W. P. Reinhardt, *Annu. Rev. Phys. Chem.* **33**, 223 (1982).
- [31] Y. K. Ho, *Phys. Rep.* **99**, 1 (1983).
- [32] F. J. Rogers, H. C. Graboske, Jr., and D. J. Harmood, *Phys. Rev. A* **1**, 1577 (1970); K. M. Roussel and R. F. O'Connell, *ibid.* **9**, 52 (1974); Y. C. Lin and Y. K. Ho (private communication).
- [33] J. M. Feagin and J. S. Briggs, *Phys. Rev. Lett.* **57**, 984 (1986); *Phys. Rev. A* **37**, 4599 (1988).